Clara, CA), was performed according to the manufacturer's instructions [19]. The data was extracted with Feature Extraction version 9 (Agilent Technologies) and visualized by CGH Analytics version 3.5 (Agilent Technologies). Statistically significant aberrations were determined using the ADM-II algorithm in CGH Analytics version 3.5 (Agilent Technologies).

3.2. Fiber-FISH analysis

Phytohemagglutinin-stimulated lymphocytes or lymphoblasts were harvested using a routine procedure that generates metaphase chromosomes and interphase nuclei. The fiber-FISH slides were prepared as follows: approximately 20 μl of cell suspensions containing metaphase and prometaphase chromosomes were pipetted onto a slide that was then dipped into a 10% sodium dodecyl sulfate (SDS) solution and removed slowly. Bacterial artificial chromosome (BAC) clones were selected from an in-silico library (UCSC Human genome browser, March 2006); RP4-540A13 and RP5-1055C14 mapped to the region surrounding *PLP1*, CTD-2171N231 and RP11-98J1 mapped to the *STS* region of Xp22.31. DNAs from the BAC clones were extracted using GenePrepStar PI-80X (Kurabo, Osaka, Japan), and labeled with digoxigenin-11-dUTP or biotin-16-dUTP (Roche Applied Science, Mannheim, Germany) by nick translation and denatured at 70 °C for 5 min. After hardening process with incubation at 65 °C for 150 min, the chromosome slides were denatured in 70% formamide/2× standard saline citrate (SSC) at 70 °C for 2 min, and then dehydrated at −20 °C in ethanol. The probe-hybridization mixture was applied on the chromosome slides and incubated at 37 °C for more than 16 h. The slides were then washed in 50% formamide/2× SSC at 37 °C for 12 min, 2× SSC at room temperature for 10 min, 1× SSC for 10 min, and 4× SSC for 10 min. And finally, the slides were incubated with 1% bovine serum albumin (BSA), 4× SSC, Fluorescein anti-biotin (Vector, Burlingame, CA, USA) and Anti-digoxigenin-rhodamine, Fab fragments (Roche) at 37 °C for 1 h. Slides were washed 3 times: in 4× SSC for 5 min, in 0.05% Triton-X-100/4× SSC for 5 min with shaking, and finally in 4× SSC for 5 min. The slides were then mounted in antifade solution containing 4′,6-diamino-2-phenylindole (DAPI) stain. Photomicroscopy was performed using a LICA CTR6000 microscope containing a quad filter set with single band excitation filters (Leica Microsystems, Tokyo, Japan).

3.3. PLP1 mutation analysis

The sequence of the patients' 7 coding exons of *PLP1* was determined using the neighboring intronic primers reported by Hobson et al. [20] and a BigDye Terminator Cycle Sequencing kit according to the manufacturer's protocol (Applied Biosystems, Foster City, CA). One hundred control samples were genotyped to verify that the *PLP1* mutation identified in the PMD patients was not found in the general population.

4. Results and discussion

4.1. Genetic diagnosis of PMD

Three distinct genetic mechanisms responsible for PMD have been reported: (1) Loss of PLP1 function caused by null mutations or deletions; (2) gain of toxic function (the PLP1 mutant protein accumulates in the endoplasmic reticulum, triggering increased oligodendrocyte cell death by apoptosis resulting in dysmyelination); (3) overexpression of PLP1 due to genomic duplication [3,7]. As mentioned in Section 2, three (P1, P3, and P4) of the 15 patients had been diagnosed as having *PLP1* duplications by previously performed comparative PCR amplification method, which were re-confirmed by aCGH and fiber-FISH in this study. Subsequently, two (P2 and P5) of the remaining twelve subjects were newly diagnosed as having *PLP1* duplications by aCGH. For the remaining ten patients without genomic duplications, we analyzed the genomic sequence of *PLP1* and identified three missense mutations, one splicing mutation, and one 3-bp deletion (Table 1). Thus, we were unable to determine genetic causes for the phenotype in the remaining five patients, and there is no patient who showed deletion of *PLP1*.

4.2. Detection of genomic duplications of PLP1 by aCGH

aCGH is a revolutionary platform that has been recently adopted in the clinical laboratory. The primary advantage of aCGH is that the array is capable of simultaneously detecting DNA copy changes at multiple loci over the whole genome [21].

In the present study, aCGH analysis identified gains of genomic copy numbers including *PLP1* in five subjects (P1, P2, P3, P4, P5), and the sizes of the chromosomal duplications were 374, 461, 676, 858, and 951-kb, respectively (Table 1 and Fig. 1a). The 461-kb duplication identified in P2 was not detected using standard FISH analysis at another medical facility previously, indicating the advantages of aCGH testing for PMD. There was no genomic copy number aberration in the remaining ten subjects (data not shown). A genomic copy number gain was identified on Xp22.31 with the size of 1.5-Mb in the sample from S1 (Fig. 1b).

4.3. Fiber-FISH analysis

aCGH holds the promise of being the initial diagnostic tool in the identification of visible and submicroscopic

Please cite this article in press as: Shimojima K et al., Comprehensive genetic analyses of *PLP1* in patients ..., Brain Dev (2009), doi:10.1016/j.braindev.2009.02.011

Table 1
Clinical characteristics of the patients with PLP1 duplications or mutations.

	P1	P2	P3	P4	P5	P6	P7	P8	P9	P10
Clinical subtype	Connatal	Classic	Connatal	Connatal	Connatal	Connatal	Connatal	Connatal	Connatal	Connatal
Age at examination	1 year	14 years	20 years	4 months	2 years	2 years	1 year	1 year	4 months	1 year 5 months
Disease onset	1 month	1 day	NA	1 day	1 month	2 months	1 day	1 week	1 month	1 month
Symptoms at onset	Nystagmus	Nystagmus	NA	Nystagmus	Nystagmus Hypotonia	Nystagmus	Asphyxia	Abnormal ABR	Microcephaly*	Nystagmus
Severity score	0	2	0	0	0	0	0	0	0	0
Family history	+	None	NA	None	None	None	None	None	None	None
Age at death				4 years						
Psychomotor development										
Head control	None	7 months	None	None	None	None	None	None	None	None
Sitting	None	4 years	None	None	None	None	None	None	None	None
Walking	None	4 years	None	None	None	None	None	None	None	None
Last evaluation	14 years	14 years	33 years	4 years	2 years	2 years	1 year	4 years	5 months	1 year 5 months
Neurological signs										
Nystagmus	+	+	None	+	+	+	+	+	+	+
Muscular hypotonia	+	None	+	+	+	+ (upper limbs)	+	+	+	+
Pyramidal signs	None	+	+		+	+ (lower limbs)	None	None	None	
Ataxia		+								
Tremor	+							+	+	Sensori-neural
Seizures				+						
deafness									Microcephaly	
Other symptoms				Choreoathetosis			Strider			
Disease course		Dysarthria Deterioration; now only sitting								
ABR findings	Only I–III waves	Only I–III waves	NA	Only I wave	Only I wave	Only I wave	Only I–III waves	Only I wave	Only I wave	Only I–II waves
MRI findings	Delayed myelination	Incomplete myelination	NA	Hypomyelination	Hypomyelination	Delayed myelination	Delayed myelination	Delayed myelination	Delayed myelination	Hypomyelination
Genotype	Duplication	Duplication	Duplication	Duplication	Duplication	Missense mutation	Missense mutation	Missense mutation	Splicing mutation	Nucleotide deletion
	374-kb	461-kb	676-kb	858-kb	951-kb	exon 2c.149A> G(p.Tyr50Cys)	exon 3c.247G> A(p.Gly83Arg)	exon 3c.254TA> Cp.Leu85Pro	intron 3IVS3-1G>C (splicing error)	exon 3c.238_240delTTC (p.Phe80del)

*, His microcephaly is −3.2SD; NA, not available; MRI, magnetic resonance imaging; ABR, auditory brain response.

Please cite this article in press as: Shimojima K et al., Comprehensive genetic analyses of *PLP1* in patients ..., Brain Dev (2009), doi:10.1016/j.braindev.2009.02.011

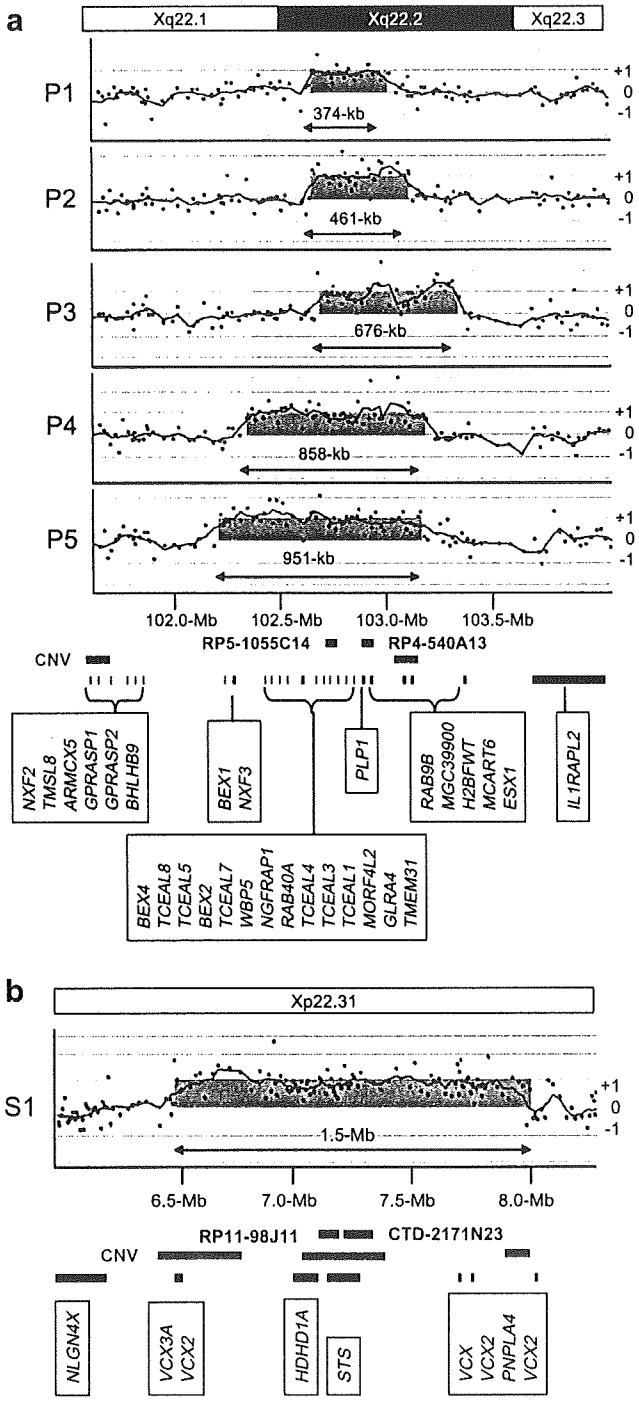

Fig. 1. Results of aCGH. CGH Analytics ver 3.5 (Agilent technologies) visualized genomic copy number aberration on Xq22.2 including *PLP1* (P1, P2, P3, P4, P5) (a) and on Xp22.31 including *STS* (S1) (b). The *X*-axis indicates physical position of chromosome X, and the scales of chromosome bands and physical position were depicted top and bottom, respectively. The *Y*-axis indicates the signal $\log_2$ ratio; positive and negative numbers indicate gain and loss of genomic copy numbers, respectively. The locations of the indicated genes (black rectangles), known copy number variations (CNVs) (orange rectangles), and the two BAC probes used in fiber-FISH analyses with green and red rectangles are shown under the figure depicted on the map according to the scale.

chromosome abnormalities [22], but it does not provide genome position or orientation information. Several cases have been reported in which the duplication is non-contiguous and the additional copy is found in a cytogenetically distinguishable band on the X chromosome (Xq22 and Xq26.3) [23]. Therefore, we should reconfirm the results of aCGH by another method including FISH analysis, especially in case of genetic counseling [23].

We checked the signals by conventional FISH analysis using metaphase, and translocations were denied in all samples (data not shown). Subsequently, two-color fiber-FISH analyses were performed to confirm the directions of the genomic duplications of *PLP1* in the five subjects, and the all duplicated segments were inserted in tandem (Fig. 2). The subjects with the longer duplicated regions (P4 and P5) showed longer intervals between the 2 sets of probe signals, which are consistent with the results of the aCGH analysis (Fig. 1a). The gain of genomic copy number on Xp22.31 in S1 was also analyzed by fiber-FISH, which showed inverted segments (Fig. 2).

Detection and visualization of *PLP1* duplications require specific molecular and cytogenetic technologies. Duplication of chromosomal regions can be determined by FISH analysis as a doublet signal in interphase chromosomes derived from immortalized lymphocyte cell lines [14,24]. However, when the duplicated region is very small and the locations of the duplicated segments are too close to each other, it is difficult to identify signals independently even if we use interphase chromosomes. In such cases, stretched chromatins rather than

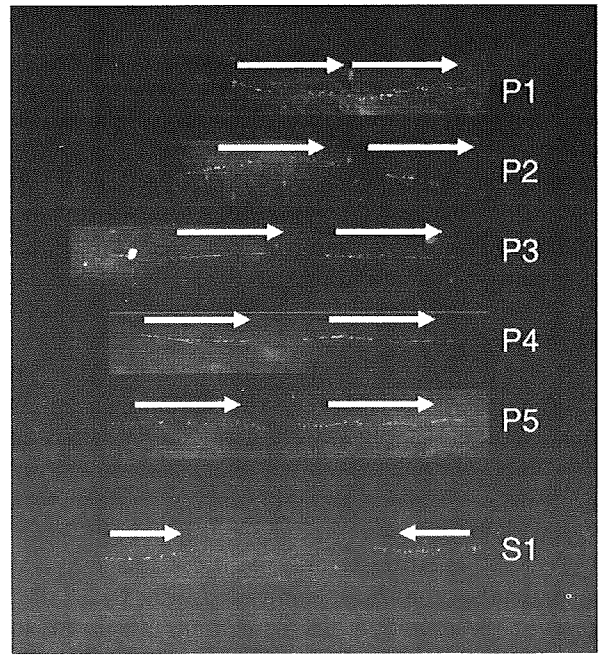

Fig. 2. The results of two-color fiber-FISH analyses. White arrows indicate the direction of duplicated segments.

Please cite this article in press as: Shimojima K et al., Comprehensive genetic analyses of *PLP1* in patients ..., Brain Dev (2009), doi:10.1016/j.braindev.2009.02.011

the conventional interphase or metaphase chromosomes can be used for fiber-FISH analysis [25]. In this technique, two copies of the gene can be visualized as a doublet signal [14].

Interestingly, in PMD patients with *PLP1* duplications, the rearrangement breakpoints for each patient are different, yielding duplicated genomic segments of varying lengths [25–28]. Based on the genomic region around *PLP1*, Woodward et al. suggest that duplicated segments or low copy repeats (LCRs) may promote instability [26]. In this study, the distal ends of the duplicated segments were located in a copy number variation (CNV) region (cnp1417: 102,969,058–103,341,717) [29] in all five subjects, and the proximal ends were differently expanded (Fig. 1a). These findings were similar to the majority of the 11 duplications found by Woodward et al. [26]. Additional studies have shown that *PLP1* duplication events may be stimulated by LCRs or by nonhomologous pairs at both the proximal and distal breakpoints [21]. Despite the variation in size, the duplications encompassing *PLP1* are usually found in tandem [26,30]. All of our subjects with *PLP1* duplications had tandem duplications, as revealed by fiber-FISH analysis (Fig. 2). We also analyzed the region of microduplications of *STS* on Xp22.31, known as the CNV region, by fiver-FISH, which demonstrated that the duplicated segment was inserted in inverted direction (Fig. 2). This indicates that the chromosomal duplication mechanism varies depending on the location.

4.4. *PLP1* mutations

To attempt to identify the genomic anomalies responsible for PMD in the remaining ten patients without *PLP1* duplications, we sequenced all the seven exons of *PLP1* and identified nucleotide alterations in five patients (Table 1, Fig. 3). Three of them were missense mutations, i.e. c.149A>G (p.Tyr50Cys) in exon 2, c.247G>A (p.Gly83Arg) in exon 3, and c.254T>C (p.Leu85Pro) in exon 3, in P6, P7, and P8, respectively. One was a splicing mutation, IVS3-1G>C in intron 3, in P9. Another was 3-bp deletion, c.238_240delCTT (p.Phe80del) in exon 3, in P10. Although c.149A>G was previously reported by Hübner et al. [18], the others were novel.

The two missense substitutions, c.247G>A and c.254T>C, are located within the second hydrophobic transmembrane domain. The nucleotide alteration, IVS3-1G>C, is located within the consensus splicing acceptor site. There is a similar known splicing mutation at the same splicing acceptor site, but it was IVS3-1G>T [31]. As PLP1 is expressed only in the central nervous system, we cannot confirm splicing alterations by RT-PCR. However, the mutations in the consensus splicing sites are believed to cause splicing abnormalities. The other novel 3-bp deletion, c.238_240delTTC, in exon 3 will cause in-frame amino acid deletion. All four novel

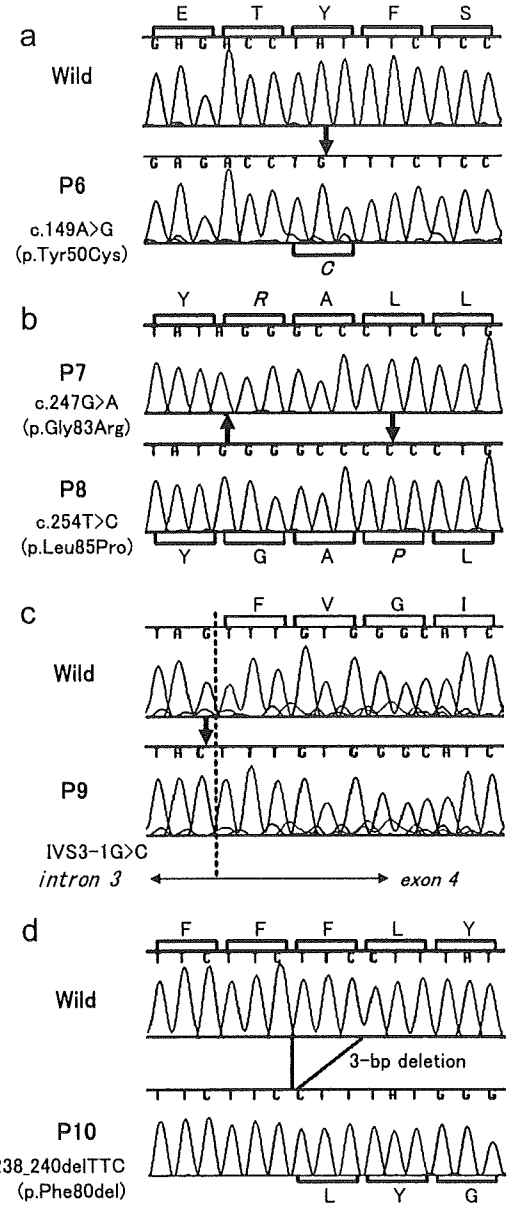

Fig. 3. Partial sequence electrophoregrams of *PLP1* mutations identified in this study. Thick arrows and italic amino acid symbols indicate the positions of mutations and altered amino acids, respectively. The broken line indicates exon–intron boundary (C). wild; sequence of wild type.

mutations were not detected in the 100 control samples, leading us to conclude that these should not be polymorphisms. Because it is well known that the genomic sequence of *PLP1* is highly conserved between species [32], these novel mutations should be pathogenic for patients with PMD. Previously, we reported two pathogenic *PLP1* mutations identified on the patients with the connatal form of PMD, and one of which, jimpy^{msd} mutation, was identical with the mice model [33,34]. Including them, more than 100 *PLP1* mutations have been reported to date (see the GeneTests Web site: http://www.genetests.org). Mutations

Please cite this article in press as: Shimojima K et al., Comprehensive genetic analyses of *PLP1* in patients ..., Brain Dev (2009), doi:10.1016/j.braindev.2009.02.011

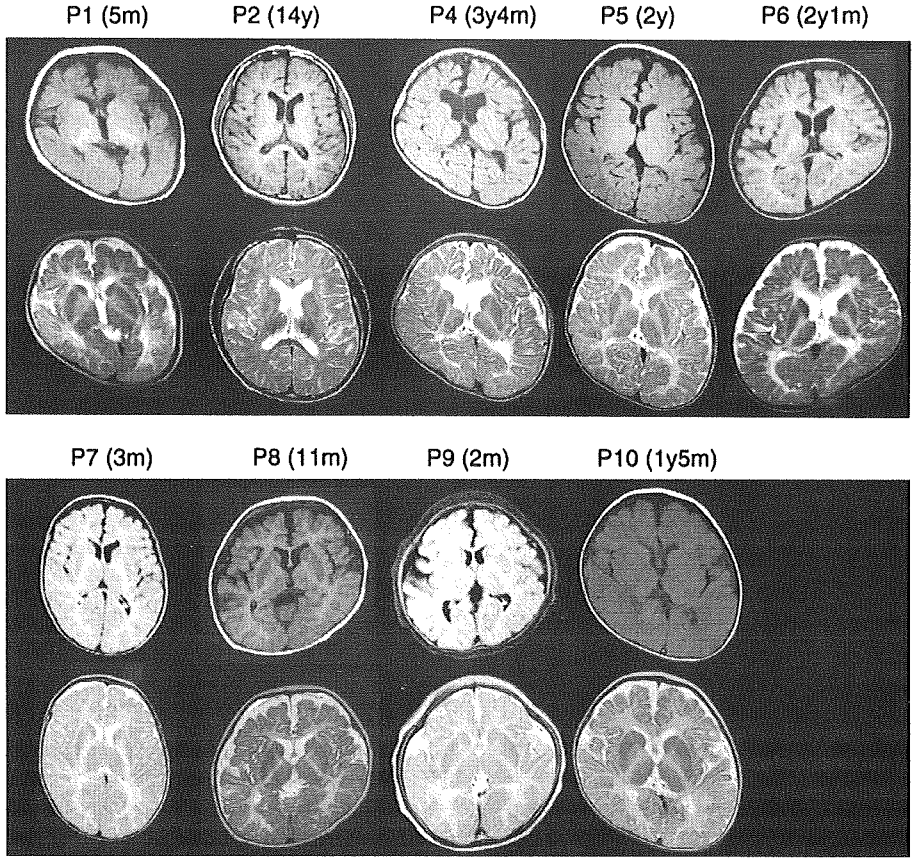

Fig. 4. Brain MRIs of nine patients analyzed in this study. Axial T1- and T2-weighted images are in the top and bottom rows, respectively. Ages at the time of examination are shown in brackets. y; years, m; months.

are distributed throughout all of the *PLP1* coding exons, and each mutation is usually unique to a family [7]. The fact that the majority of *PLP1* missense mutations cause more severe phenotypes than null mutations suggests that the profound dysmyelination resulting from *PLP1* point mutations probably arises not from the absence of functional protein, but rather from a cytotoxic effect of the mutant protein [3].

4.5. Correlation of PLP1 genotypes with PMD phenotypes

The clinical phenotypes of ten subjects who were diagnosed as having *PLP1* duplications (five) or *PLP1* nucleotide alterations (five) are summarized in Table 1. P2 is the only patient with the milder classic form of PMD, and demonstrated the greatest walking ability of all cases in this study. The other subjects were diagnosed with the connatal form of PMD with severe developmental delay. P4 died at age 4, although no details were provided.

Brain MRIs were obtained from nine patients and shown in Fig. 4. All of them showed abnormal intensity in the white matter. Although P2 showed normal high intensity in T1-weighted image (T1), that of the frontal lobe in T2-weighted image (T2) is higher than that of the occipital. This indicated incomplete myelination. P6, P7, P8, and P9 showed high intensity in both T1 and T2, indicating delayed myelination. P1 showed low intensity in T1, and high intensity in T2. As these MRIs were obtained when he was 5 months old, this indicated delayed myelination. P4, P5, and P10 showed low intensity in T1, and high intensity in T2, indicating very severe hypomyelination.

All ten patients having a *PLP1* mutation or duplication showed nystagmus in early infancy, dysmyelination revealed by MRI, and auditory brain response (ABR) abnormalities (Table 1). This triad of presenting symptoms should be the clue to get a clinical diagnosis of PMD. Regarding the radiological findings of the patients, all the provided MRI findings showed dysmyelination with varying degrees (Fig. 4). P4 with the most severe phenotype of PMD showed very low intensity white matter in the T1-weighted imaging, whereas P2 with the mildest form of PMD showed only mildly affected incomplete myelination in T2-weighted imaging. These MRI findings are well-correlated with the clinical severity.

All five patients with nucleotide alterations in *PLP1* displayed the very severe connatal type PMD, whereas P2 whose genome contained a small duplication including *PLP1* showed the milder classical type PMD. These results agree with previous reports showing that the phe-

Please cite this article in press as: Shimojima K et al., Comprehensive genetic analyses of *PLP1* in patients ..., Brain Dev (2009), doi:10.1016/j.braindev.2009.02.011

notypes of patients with genomic duplications are generally milder than those with nucleotide mutations [3]. However, the other four patients with *PLP1* duplications, P1, P3, P4, and P5, displayed the severe connatal form of PMD.

P4 showed a large duplicated region and died when he was 4 years old. On the other hand, P1 contained a very small duplicated segment, similar to P2 in the length, but displayed a very severe phenotype. Thus, it appears that, as suggested by Regis et al., the extent of the duplicated genomic segments does not correlate with clinical severity [35].

According to Lee et al., 65% of patients with *PLP1* duplications have complex rearrangements in nucleotide sequence levels [28]. In this study, we detected *PLP1* duplications by aCGH, and the directions of those duplicated regions were determined by fiber-FISH. However, there is still the possibility that more complicated small rearrangements exist in the duplicated region, particularly in P1. The existence of more complicated rearrangements may explain the reason why there is no correlation between the size of the duplication and the phenotypic severity.

4.6. Differential diagnosis

After genetic evaluation of *PLP1*, the five patients, who did not show any mutations in *PLP1*, were re-evaluated, and one of them was diagnosed as having metachromatic leukodystrophy in the other institution. Another patient showed congenital leukodystrophy with migrating partial seizures in infancy, but no nystagmus and no ABR abnormality, indicating that PMD would be misdiagnosis. Since the other three patients fulfilled the triad described above, the disease-causing mutations might be on the non-coding upstream region of PLP1, or on the other candidate genes for congenital leukodystrophy, including the gap junction protein α12 (GJA12) and others [36,37].

Acknowledgements

This work was supported by the International Research and Educational Institute for Integrated Medical Sciences, Tokyo Women's Medical University, which is supported by the Program for Promoting the Establishment of Strategic Research Centers, Special Coordination Funds for Promoting Science and Technology, Ministry of Education, Culture, Sports, Science and Technology (Japan).

References

[1] Boulloche J, Aicardi J. Pelizaeus–Merzbacher disease: clinical and nosological study. J Child Neurol 1986;1:233–9.
[2] Koeppen AH, Robitaille Y. Pelizaeus–Merzbacher disease. J Neuropathol Exp Neurol 2002;61:747–59.
[3] Inoue K. PLP1-related inherited dysmyelinating disorders: Pelizaeus–Merzbacher disease and spastic paraplegia type 2. Neurogenetics 2005;6:1–16.
[4] Hudson LD, Puckett C, Berndt J, Chan J, Gencic S. Mutation of the proteolipid protein gene PLP in a human X chromosome-linked myelin disorder. Proc Natl Acad Sci USA 1989;86:8128–31.
[5] Gencic S, Abuelo D, Ambler M, Hudson LD. Pelizaeus–Merzbacher disease: an X-linked neurologic disorder of myelin metabolism with a novel mutation in the gene encoding proteolipid protein. Am J Hum Genet 1989;45:435–42.
[6] Ellis D, Malcolm S. Proteolipid protein gene dosage effect in Pelizaeus–Merzbacher disease. Nat Genet 1994;6:333–4.
[7] Garbern JY. Pelizaeus–Merzbacher disease: genetic and cellular pathogenesis. Cell Mol Life Sci 2007;64:50–65.
[8] Heim P, Claussen M, Hoffmann B, Conzelmann E, Gartner J, Harzer K, et al. Leukodystrophy incidence in Germany. Am J Med Genet 1997;71:475–8.
[9] Cailloux F, Gauthier-Barichard F, Mimault C, Isabelle V, Courtois V, Giraud G, et al. Genotype-phenotype correlation in inherited brain myelination defects due to proteolipid protein gene mutations. Clinical European network on brain dysmyelinating disease. Eur J Hum Genet 2000;8:837–45.
[10] Sistermans EA, de Coo RF, De Wijs IJ, Van Oost BA. Duplication of the proteolipid protein gene is the major cause of Pelizaeus–Merzbacher disease. Neurology 1998;50:1749–54.
[11] Mimault C, Giraud G, Courtois V, Cailloux F, Boire JY, Dastugue B, et al. Proteolipoprotein gene analysis in 82 patients with sporadic Pelizaeus–Merzbacher disease: duplications, the major cause of the disease, originate more frequently in male germ cells, but point mutations do not. The clinical European network on brain dysmyelinating disease. Am J Hum Genet 1999;65:360–9.
[12] Caro PA, Marks HG. Magnetic resonance imaging and computed tomography in Pelizaeus–Merzbacher disease. Magn Reson Imaging 1990;8:791–6.
[13] Inoue K, Osaka H, Sugiyama N, Kawanishi C, Onishi H, Nezu A, et al. A duplicated PLP gene causing Pelizaeus–Merzbacher disease detected by comparative multiplex PCR. Am J Hum Genet 1996;59:32–9.
[14] Woodward K, Kendall E, Vetrie D, Malcolm S. Pelizaeus–Merzbacher disease: identification of Xq22 proteolipid-protein duplications and characterization of breakpoints by interphase FISH. Am J Hum Genet 1998;63:207–17.
[15] Wolf NI, Sistermans EA, Cundall M, Hobson GM, Davis-Williams AP, Palmer R, et al. Three or more copies of the proteolipid protein gene PLP1 cause severe Pelizaeus–Merzbacher disease. Brain 2005;128:743–51.
[16] Combes P, Bonnet-Dupeyron MN, Gauthier-Barichard F, Schiffmann R, Bertini E, Rodriguez D, et al. PLP1 and GPM6B intragenic copy number analysis by MAPH in 262 patients with hypomyelinating leukodystrophies: identification of one partial triplication and two partial deletions of PLP1. Neurogenetics 2006;7:31–7.
[17] Lee JA, Cheung SW, Ward PA, Inoue K, Lupski JR. Prenatal diagnosis of PLP1 copy number by array comparative genomic hybridization. Prenat Diagn 2005;25:1188–91.
[18] Hubner CA, Orth U, Senning A, Steglich C, Kohlschutter A, Korinthenberg R, et al. Seventeen novel PLP1 mutations in patients with Pelizaeus–Merzbacher disease. Hum Mutat 2005;25:321–2.
[19] Bartocci A, Striano P, Mancardi MM, Fichera M, Castiglia L, Galesi O, et al. Partial monosomy Xq(Xq23 –> qter) and trisomy 4p(4p15.33 –> pter) in a woman with intractable focal epilepsy, borderline intellectual functioning, and dysmorphic features. Brain Dev 2008;30:425–9.
[20] Hobson GM, Davis AP, Stowell NC, Kolodny EH, Sistermans EA, de Coo IF, et al. Mutations in noncoding regions of the proteolipid protein gene in Pelizaeus–Merzbacher disease. Neurology 2000;55:1089–96.

Please cite this article in press as: Shimojima K et al., Comprehensive genetic analyses of *PLP1* in patients ..., Brain Dev (2009), doi:10.1016/j.braindev.2009.02.011

[21] Bejjani BA, Shaffer LG. Application of array-based comparative genomic hybridization to clinical diagnostics. J Mol Diagn 2006;8:528–33.
[22] Shaffer LG, Bejjani BA. Medical applications of array CGH and the transformation of clinical cytogenetics. Cytogenet Genome Res 2006;115:303–9.
[23] Woodward K, Cundall M, Palmer R, Surtees R, Winter RM, Malcolm S. Complex chromosomal rearrangement and associated counseling issues in a family with Pelizaeus–Merzbacher disease. Am J Med Genet A 2003;118A:15–24.
[24] Inoue K, Kanai M, Tanabe Y, Kubota T, Kashork CD, Wakui K, et al. Prenatal interphase FISH diagnosis of PLP1 duplication associated with Pelizaeus–Merzbacher disease. Prenat Diagn 2001;21:1133–6.
[25] Inoue K, Osaka H, Imaizumi K, Nezu A, Takanashi J, Arii J, et al. Proteolipid protein gene duplications causing Pelizaeus–Merzbacher disease: molecular mechanism and phenotypic manifestations. Ann Neurol 1999;45:624–32.
[26] Woodward KJ, Cundall M, Sperle K, Sistermans EA, Ross M, Howell G, et al. Heterogeneous duplications in patients with Pelizaeus–Merzbacher disease suggest a mechanism of coupled homologous and nonhomologous recombination. Am J Hum Genet 2005;77:966–87.
[27] Lee JA, Inoue K, Cheung SW, Shaw CA, Stankiewicz P, Lupski JR. Role of genomic architecture in PLP1 duplication causing Pelizaeus–Merzbacher disease. Hum Mol Genet 2006;15:2250–65.
[28] Lee JA, Carvalho CM, Lupski JR. A DNA replication mechanism for generating nonrecurrent rearrangements associated with genomic disorders. Cell 2007;131:1235–47.
[29] Redon R, Ishikawa S, Fitch KR, Feuk L, Perry GH, Andrews TD, et al. Global variation in copy number in the human genome. Nature 2006;444:444–54.
[30] Inoue K. Pelizaeus–Merzbacher disease and spastic paraplegia type 2. In: Lupski JR, Stankiewicz P, editors. Genomic disorders. Totowa, NJ: Humana press; 2006. p. 263–9.
[31] Strautnieks S, Malcolm S. A G to T mutation at a splice site in a case of Pelizaeus–Merzbacher disease. Hum Mol Genet 1993;2:2191–2.
[32] Diehl HJ, Schaich M, Budzinski RM, Stoffel W. Individual exons encode the integral membrane domains of human myelin proteolipid protein. Proc Natl Acad Sci USA 1986;83:9807–11.
[33] Yamamoto T, Nanba E, Zhang H, Sasaki M, Komaki H, Takeshita K. Jimpy(msd) mouse mutation and connatal Pelizaeus–Merzbacher disease. Am J Med Genet 1998;75:439–40.
[34] Yamamoto T, Nanba E. A novel mutation (A246T) in exon 6 of the proteolipid protein gene associated with connatal Pelizaeus–Merzbacher disease. Hum Mutat 1999;14:182.
[35] Regis S, Biancheri R, Bertini E, Burlina A, Lualdi S, Bianco MG, et al. Genotype-phenotype correlation in five Pelizaeus–Merzbacher disease patients with PLP1 gene duplications. Clin Genet 2008;73:279–87.
[36] Uhlenberg B, Schuelke M, Ruschendorf F, Ruf N, Kaindl AM, Henneke M, et al. Mutations in the gene encoding gap junction protein alpha 12 (connexin 46.6) cause Pelizaeus–Merzbacher-like disease. Am J Hum Genet 2004;75:251–60.
[37] Henneke M, Combes P, Diekmann S, Bertini E, Brockmann K, Burlina AP, et al. GJA12 mutations are a rare cause of Pelizaeus–Merzbacher-like disease. Neurology 2008;70:748–54.

Please cite this article in press as: Shimojima K et al., Comprehensive genetic analyses of *PLP1* in patients ..., Brain Dev (2009), doi:10.1016/j.braindev.2009.02.011

ELSEVIER

Brain & Development 31 (2009) 248–251

BRAIN & DEVELOPMENT
Official Journal of the Japanese Society of Child Neurology

www.elsevier.com/locate/braindev

Case report

A novel *PLP* mutation in a Japanese patient with mild Pelizaeus-Merzbacher disease

Tetsuya Kibe [a,*], Jun Miyahara [a], Kenji Yokochi [a], Akiko Iwaki [b]

[a] *Department of Pediatrics and Pediatric neurology, Seirei-Mikatahara General Hospital, 3453 Mikatahara, Hamamatsu, Shizuoka 433-8558, Japan*
[b] *Division of Human Molecular Genetics, Research Center for Genetic Information, Medical Institute of bioregulation, Kyusyu University, Fukuoka, Japan*

Received 13 February 2008; received in revised form 28 July 2008; accepted 2 August 2008

Abstract

Pelizaeus-Merzbacher disease (PMD) is a rare dysmyelinating disorder due to mutations in the proteolipid protein (*PLP*) gene. *PLP* gene mutations are responsible for a broad spectrum of disease, from the most severe form, connatal PMD, to a less severe form, spastic paraplegia 2 (SPG2). We describe here a very mild case of PMD in a patient who presented with nystagmus in early infancy and was unable to walk until 1 year 7 months of age. Brain magnetic resonance imaging (MRI) at 1 year 7 months of age revealed white matter abnormalities typical of PMD. Genetic testing revealed a novel mutation of the *PLP* gene (Gly197Arg). The patient presented with only mildly ataxic gait and slurred speech at the age of 4 years. Gly197Arg is the first novel mutation located within exon 4 of the *PLP* gene and associated with mild PMD/SPG2 in a Japanese patient.

Keywords: Pelizaeus-Merzbacher disease; Mild phenotype; Novel *PLP* point mutation

1. Introduction

Pelizaeus-Merzbacher Disease (PMD) is an X-linked recessive neurological disorder characterized by abnormal myelination (hypomyelination or dysmyelination) and death of oligodendroglia in the central nervous system (CNS) [1,2].

Three major clinical forms of PMD are classified by age of onset and severity of disease: connatal, transitional, and classical [1,2]. Classical PMD, which usually features onset in early infancy, typically manifests as horizontal nystagmus associated with a head tremor. Motor development progresses slowly, with the eventual onset of spasticity, ataxia, and involuntary movements. Typically, disease progression slows toward the middle or end of the first decade, with death occurring in adolescence or early adulthood. Connatal PMD presents shortly after birth, with severe hypotonia, stridor, feeding difficulties, and marked spasticity resulting in multiple contractures. Patients usually die within the first decade of life. Transitional PMD has a clinical presentation that often combines features of both the classic and connatal types.

PMD is caused by mutations in the proteolipid protein (*PLP*) gene, the products of which, PLP and its isoform DM20, are major components of myelin sheath. Mutation of the *PLP* gene also causes spastic paraplegia 2 (SPG2), which has been considered the mildest phenotype of PMD. Previous studies have revealed that the most common mutation in PMD is gene duplication (50–70%), though missense mutations (~20%), insertions, and deletions have been identified as well [1,2]. More than 100 different mutations of the *PLP* gene have

* Corresponding author. Address: Department of Pediatrics, Seirei-Mikatahara General Hospital, 3453 Mikatahara, Hamamatsu, Shizuoka 433-8558, Japan. Tel.: +81 53 436 1251; fax: +81 53 438 0652.
E-mail address: tkmn3994@yahoo.co.jp (T. Kibe).

0387-7604/$ - see front matter © 2008 Elsevier B.V. All rights reserved.
doi:10.1016/j.braindev.2008.08.001

been detected (http://www.hgmd.cf.ac.uk/ac/index.php). Several studies on genotype-phenotype correlation in PMD have demonstrated effects of the type and location of mutation of the *PLP* gene on phenotype [3–5].

We describe here a case of a very mild form of PMD/SPG2 in which, despite early onset of disease and brain MRI findings consistent with typical classical PMD, the clinical course has been very mild. Genetic testing revealed a novel mutation (Gly197Arg) of the *PLP* gene in this patient.

2. Case report

The patient was born after an uncomplicated 41-week gestation period. He was the second child of non-consanguineous, healthy Japanese parents. His 4-year-old sister and 5-year-old maternal cousin are also healthy. At 3 months of age, he was observed to have horizontal nystagmus, and was tentatively diagnosed with congenital nystagmus at a local clinic. Developmental milestones in infancy were considered to be within normal range; for example, he could crawl at 7 months, sit unassisted at 8 months, and walk with help at 12 months of age. Thereafter, his development was retarded, and he was unable to walk until 1 year 7 months of age, when he was referred to our hospital for evaluation of developmental delay. Neurological examination revealed slightly decreased muscle tone and mild ataxia on standing. Mental development appeared normal. Brain MRI at 1 year 8 months of age revealed signal increase only in the white matter of the central sulcus, optic radiation, and corona radiata on T1-weighted images, evaluated as a level of myelination typical of the neonatal period to early infancy. Results of blood chemistry tests were all within normal range. Brainstem auditory-evoked potentials revealed increase in wave V latency (6.78 ms. in the right ear and 6.86 ms. in the left ear; normal range, 6.02 ± 0.28).

Molecular genetic analyses were performed at 1 year 9 months of age as described previously [6] after informed consent was obtained from his parents. Direct sequencing of the patient's DNA revealed a G–C change at nucleotide 589 in exon 4 of the *PLP* gene. This mutation is expected to result in a Gly197Arg amino acid change in the second extracellular domain of the PLP protein. This mutation was absent in one hundred normal alleles. It is thus unlikely that the G–C substitution represents a common polymorphism in the Japanese population. Other family members were not available for testing.

Thereafter, his condition improved clinically, and he could walk alone with mild ataxia at 2 year 8 months of age. However, follow-up MRI at that time revealed no remarkable improvement of myelination (Fig. 1). By 3 years 1 months of age, his nystagmus had completely disappeared. On neurological examination, he had mild ataxia of the extremities. Limb deep tendon reflexes were not increased. At 4 years 2 months of age, he could run, jump, and stand on one leg. Although he had mild dysarthria (slurred speech), his speech function was comprehensive.

3. Discussion

Based on the patient's early clinical course and MRI findings, we suspected PMD and identified a novel mutation, Gly197Arg, in exon 4 of the *PLP* gene. Although he did exhibit a phase of developmental delay in early childhood, his only recognizable signs of PMD are mild ataxia and slurred speech, without apparent spasticity at the age of four. This patient differs from most PMD patients in that he is improving clinically.

The mutation found in our patient, Gly197Arg in exon 4, has not been previously described (http://www.hgmd.cf.ac.uk/ac/index.php). This mutation results in substitution of a non-conserved amino acid within the second extracellular loop. This substitution, introducing a side chain with a net positive charge, may have deleterious effects on protein function. Patients with mild phenotypes of PMD have previously been reported in association with a variety of mutations [1,2]. Cailloux et al. [5] found that the absence of PLP/DM20, PLP-specific mutations, and substitutions of non-conserved amino acids in the second extracellular loop were responsible for the mildest form of PMD, which is clinically similar to complex forms of SPG2. These findings are compatible with those in the present case. The cellular basis for the range of severity of PMD is not completely understood, but is probably related to differences in the cellular effects of individual PLP mutations [1,2]. In general, more severe abnormalities of protein folding or conformational changes in the protein (PLP/DM20) at locations of key chemical interactions result in more severe phenotypes. Most symptomatic children have abnormalities in the large protein loop that is in the extracellular space and interacts with the adjacent myelin spiral. In addition to the obvious effects that such changes will have on the physical structure of myelin, it has been suggested that misfolded proteins are less easily transported to the cell membrane from the endoplasmic reticulum (ER) of oligodendroglial cells. The accumulation of misfolded proteins in the ER may trigger oligodendroglial apoptosis and consequent demyelination. Gow et al. [7] revealed that mutations affecting the folding of both PLP and DM20 are associated with the most severe PMD phenotypes, and also cause increased oligodendrocyte cell death. However, mutations that affect the transport of PLP but not of DM20 produce less severe PMD phenotypes, and do not cause increased oligodendrocyte cell death. Koizume et al. [8] demonstrated that a transfected

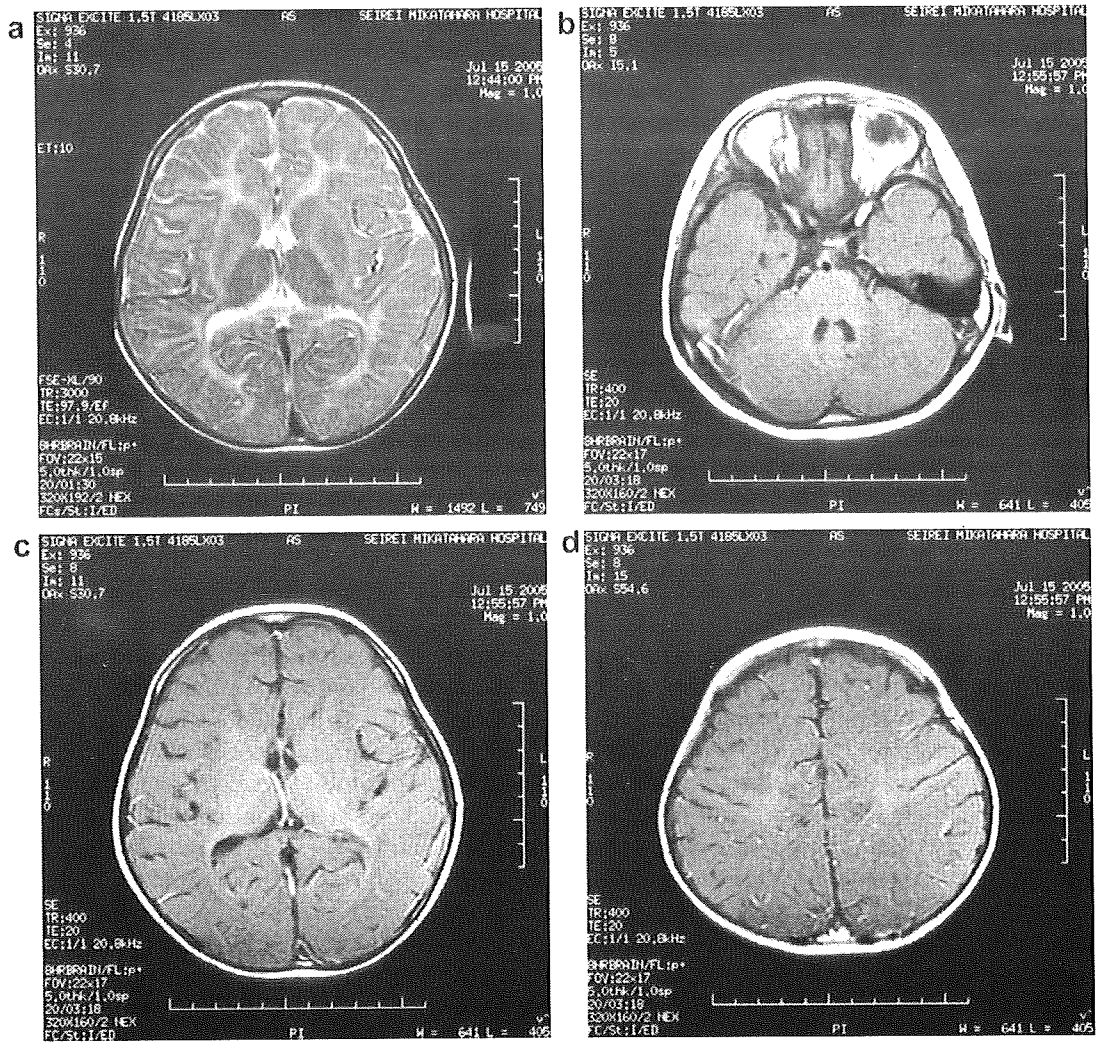

Fig. 1. (a) Axial T2-weighted MR image at 2 years 8 months of age. A diffuse, symmetric signal abnormality involving most of the cerebral white matter is noted, with sparing of small portions of the posterior limbs of the internal capsule. (b–d) Axial T1 image at 2 years 8 months of age. Signal increase is present in the basilar region of the pons, inferior and middle cerebellar peduncles, and part of the cerebellar white matter (b). The corona radiata and optic radiation exhibit signal increase. The posterior limbs of the internal capsule exhibit no signal increase (c). Mild signal increase is noted in the central sulcus (d).

mutant PLP, which had a mutation associated with mild phenotype, Trp162Leu, escaped trapping in the ER and accumulated in the nuclear membrane. This might be one of the cellular bases of the mild phenotype. The mutation found in our case might also be related to escape of PLP/DM20 from accumulation in ER.

MR imaging of PMD generally reveals either diffuse or patchy (tigroid) T2-hyperintensity in both the supra- and subtentorial white matter [9]. This appearance is believed to be the result of the lack of formation of myelin. Diffuse confluent involvement is usually observed in the severe connatal form, whereas the tigroid pattern is more common in patients with mild forms of PMD/SPG2. Atrophy and decreased white matter volume may also be noted. In addition to lack of myelination, axonal degeneration has recently been shown to occur in PMD, which may be in part responsible for the disability observed in patients with this disease [1,2]. Our patient had abnormal imaging findings with fairly significant white matter signal change indicative of severe abnormalities even at the age of 2 year and 8 months, when he could walk alone with mild ataxia. However, follow-up at 3 years after imaging studies unexpectedly revealed very mild phenotype with some clinical improvement. Thus, at least in this patient, early imaging abnormalities did not correlate with a worse neurological outcome. Further studies are needed to establish the relationships between findings of imaging and the severity of PMD.

In conclusion, we experienced a patient with a very mild form PMD/SPG2. The existence of very mild forms of PMD/SPG2 should be considered even when a patient exhibits only mild ataxia.

Acknowledgement

This work was supported in part by a grant-in-Aid for General Scientific Research from the Ministry of Education, Culture, Sports, Science, and Technology of Japan.

References

[1] Inoue K. PLP1-related inherited dysmyelinating disorders: Pelizaeus-Merzbacher disease and spastic paraplegia type 2. Neurogenetics 2005;6:1–16.
[2] Garbern JY. Pelizaeus-Merzbacher disease: genetic and cellular pathogenesis. Cell Mol Life Sci 2007;64:50–65.
[3] Sistermans EA, de Coo RF, De Wijis IJ, Van Oost BA. Duplication of proteolipid protein gene is the major cause of Pelizaeus-Merzbacher disease. Neurology 1998;50:1749–54.
[4] Hodes ME, Zimmerman AW, Aydanian A, Naidu S, Miller NR, Garcia Oller JL, et al. Different mutations in the same codon of the proteolipid protein gene, PLP, may help in correlating genotype with phenotype in Pelizaeus-Merzbacher disease/X-linked spastic paraplegia (PMD/SPG2). Am J Med Genet 1999;82:132–9.
[5] Cailloux F, Gauthier-Barichard F, Mimault C, Isabelle V, Courtois V, Giraud G, et al. Genotype-phenotype correlation in inherited brain myelination defects due to proteolipid protein gene mutations. Clinical European network on brain dysmyelinating disease. Eur J Hum Genet 2000;8:837–45.
[6] Iwaki A, Muramoto T, Iwaki I, Furumi H, Dario-deLeon ML, Tateishi J, et al. A missense mutation in the proteolipid protein gene responsible for Pelizaeus-Merzbacher disease in a Japanese family. Hum Mol Genet 1993;2:19–22.
[7] Gow A, Lazzarini RA. A cellular mechanism governing the severity of Pelizaeus-Merzbacher disease. Nat Genet 1996;13:422–8.
[8] Koizume S, Takizawa S, Fujita K, Aida N, Yamashita S, Miyagi Y, et al. Aberrant trafficking of a proteolipid protein in a mild Pelizaeus-Merzbacher disease. Neuroscience 2006;141:1861–9.
[9] Nezu A, Kimura S, Takeshita S, Osaka H, Kimura K, Inoue K. An MRI and MRS study of Pelizaeus-Merzbacher disease. Pediatr Neurol 1998;18:334–7.

ELSEVIER

Brain & Development 31 (2009) 582–587

BRAIN & DEVELOPMENT
Official Journal of the Japanese Society of Child Neurology

www.elsevier.com/locate/braindev

Original article

Diffuse cerebral hypomyelination with cerebellar atrophy and hypoplasia of the corpus callosum

Masayuki Sasaki [a,*], Jun-ichi Takanashi [c], Hiroko Tada [d], Hiroshi Sakuma [a], Wakana Furushima [a], Noriko Sato [b]

[a] *Department of Child Neurology, National Center of Neurology and Psychiatry (NCNP), 4-1-1 Ogawahigashi-cho Kodaira, Tokyo 187-8551, Japan*
[b] *Department of Radiology, NCNP, Tokyo, Japan*
[c] *Department of Pediatrics, Kameda Medical Center, Kamogawa, Japan*
[d] *Segawa Neurological Clinic for Children, Tokyo, Japan*

Received 22 February 2008; received in revised form 4 August 2008; accepted 5 September 2008

Abstract

Three unrelated Japanese patients who presented with ataxia and mild mental retardation were examined in this study. Early development was normal in two patients and slightly delayed in one. All could walk independently, but were unstable due to cerebellar ataxia. They had mild intellectual retardation and displayed slow, progressive, and mild clinical courses. Two patients lost the ability to walk at 12 and 25 years of age. Brain MRI of the three patients revealed diffuse cerebral hypomyelination, moderate cerebellar cortical atrophy, and hypoplasia of the corpus callosum, which were seen in other diffuse hypomyelination syndrome. No known abnormalities were found in biochemical and genetic studies. Auditory brainstem responses and nerve conduction studies were normal. A definite diagnosis could not be made because of the lack of hypodontia, hypogonadism, cataracts, or basal ganglia atrophy. Based on common MRI findings and the relatively mild clinical courses, we believe that these patients may have another subset form of diffuse hypomyelination syndrome involving the cerebral white matter and cerebellum.

Keywords: Hypomyelination; Cerebellar atrophy; Atrophy of the corpus callosum; Slow progressive; MRI

1. Introduction

Recent advances in magnetic resonance imaging (MRI) have made it easy to recognize the presence of cerebral white matter disorders. However, despite extensive investigations, more than half of young patients with cerebral white matter disorders cannot be diagnosed correctly [1]. van der Knaap et al. [1] successfully divided abnormalities of cerebral white matter into several categories using MRI. Several new syndromes involving cerebral white matter have been described recently. Childhood ataxia with diffuse central nervous system hypomyelination was consistent with vanishing white matter leukoencephalopathy [2,3]. Leukoencephalopathy with swelling and a discrepantly mild clinical course was named megalencephalic leukoencephalopathy with subcortical cysts [4]. Genetic abnormalities were discovered in both disorders [5,6]. A new syndrome characterized by hypomyelination with atrophy of the basal ganglia and cerebellum (H-ABC) was also proposed by van der Knaap et al. [7]; the underlying genetic abnormality responsible for this entity has not been identified [8–10]. Other new syndromes involving diffuse hypomyelination with systemic abnormalities such as cataracts, hypogonadism, and/or hypodontia have also been reported [11–15].

* Corresponding author. Tel.: +81 42 341 2711; fax: +81 42 344 6745.
E-mail address: masasaki@ncnp.go.jp (M. Sasaki).

0387-7604/$ - see front matter © 2008 Elsevier B.V. All rights reserved.
doi:10.1016/j.braindev.2008.09.003

We describe three unrelated cases with common brain MRI findings including supratentorial diffuse hypomyelination, cerebellar atrophy, and hypoplasia of the corpus callosum, and relatively mild clinical courses.

2. Patients and methods

Clinical histories for each patient are presented in Table 1.

Patient 1 was an 11-years-old female. She was born to healthy and unrelated parents after an uneventful delivery, and had a healthy younger brother. Early developmental milestones were normal. She obtained head control at 3 months, sat without support at 6 months, and walked without support at 11 months. She started to speak words at 18 months and sentences at 2 years of age. Her parents noted that she walked unsteadily from the time she began to walk, and that she fell down easily. The patient came to our hospital at 4 years of age. She had ataxic gait, dysarthria, intention tremor, and dysmetria. She also had a mild intellectual disability. At 11 years of age, she showed no further deterioration. She had a short stature (119 cm; −3 SD), normal head circumference, and cerebral symptoms (mild spasticity and intellectual disability). Teeth were normal, and blood examination revealed normal gonadotropin levels.

Patient 2 was a 16-years-old male. He was born to healthy and unrelated parents after an uneventful delivery. Early development was normal. He began to walk when he was 12 months old, but his walking remained unstable from the time he began walking. He spoke several words from 1 year of age, and simple sentences from 3 years of age. He lost the ability to walk at 12 years of age. At 16 years of age, he showed increasing muscle tone and exaggerated deep tendon reflexes. Pathological reflexes were positive. He could not maintain an upright position, and had tremors and dysmetria in the upper extremities. Motor deterioration was prominent, but intellectual disability was not progressive.

Patient 3 was a 33-years-old male. He was born to healthy and unrelated parents after an uneventful delivery. He achieved steady head control at 4 months of age, and could roll over at 7 months. He could walk without support at 2 years and 4 months of age, but tended to walk unsteadily. The patient was diagnosed with ataxic cerebral palsy at 3 years of age. He was able to speak several words from the age of 2 years, and could construct sentences from 6 years of age. He attended a school for physically handicapped children for 12 years. Motor and intellectual deterioration started after 20 years of age. He lost the ability to walk by 25 years of age, and gradually lost the ability to speak words. He developed tonic seizures at 27 years of age, and was

Table 1
Clinical history and present findings in the patients

	Patient 1	Patient 2	Patient 3
Current age (Y)	11	16	33
Sex	Female	Male	Male
Consanguinity	No	No	No
Initial motor development	Normal	Normal	Delayed
Unsupported walking	11 months unsteady	12 months unsteady	2 year 4 months unsteady
Onset of motor deterioration	No deterioration	10 Years	20 Years
Loss of walking	Still able to walk	12 Years	25 Years
Motor signs			
Ataxia	Yes	Yes	Yes
Tremor	Yes	Yes	Yes
Choreoathetosis	No	No	No
Dystonia	No	Yes	Yes
Spasticity	Yes	Yes	Yes
Rigidity	No	Yes	Yes
Dysarthria	Yes	Yes	Yes
Nystagmus	No	No	No
Intelligence	MR (mild)	MR (mild)	MR (moderate)
Cognitive decline	No	Yes	Yes
Epilepsy	No	No	Yes: Few seizures
Vision	Normal	Normal	Normal
Hearing	Normal	Normal	Normal
HC	Normal	Normal	Normal
Stature	<2SD	Normal	Normal
Hypogonadism	No	No	No
Hypodontia	No	No	No
Cataract	No	No	No

HC, head circumference; MR, mental retardation.

successfully treated with carbamazepine. At 33 years of age, he showed increasing muscle tone and exaggerated deep tendon reflexes. Pathological reflexes were positive. He could sit, but not move, by himself, and had tremors and dysmetria in the upper extremities. The patient also exhibited spasticity and mild dystonia.

All patients underwent biochemical studies of blood and urine, genetic analysis, neurophysiological examination. MRI and proton magnetic resonance spectroscopy (MRS) were performed with 1.5T. Conventional T1- and T2-weighted images were obtained in axial and coronal section. Sagittal section was done only in T1-weighted image. MRS of the cerebral white matter was performed.

3. Results

3.1. Laboratory findings

Patients underwent the following tests: blood gas analysis; blood lactate/pyruvate analysis; sialic acid analysis; protein-C and protein-S tests; very long-chain fatty acid analysis (blood); lymphocyte lysosomal enzyme activities (arylsulfatase A, beta galactosidase, and hexosaminidase A); amino acid analysis (plasma); and organic acid analysis (urine). No abnormal results were obtained.

Genetic analyses of the proteolipid protein (*PLP*) and gap junction protein (*GJP12*) for Pelizaeus-Merzbacher disease did not reveal abnormalities. Karyotypic analysis of blood cells did not reveal abnormalities, and showed that there were no deletions in chromosome 18.

Brainstem auditory evoked potentials were recorded, and the latencies of waves I–V were found to be normal in all patients. Nerve conduction velocities and the amplitudes of compound muscle action potentials were also within normal limits.

3.2. MRI

A complete lack of myelin throughout the supratentorial cerebral white matter was observed in all cases in T2-weighted images (Fig. 1a–c). In T1-weighted images, myelin in the cerebral white matter in patients 2 and 3 seemed almost normal (data not shown). The brainstem and cerebellar white matter contained some myelin in T2-weighted images. The corpus callosum was very thin, and was normally myelinated in T1-weighted images in all patients (Fig. 1d–f). Diffuse cerebellar atrophy, particularly in the cortex, was observed in all patients (Figs. 1 and 2). Pons was slightly atrophic in all (Fig. 2). T2-weighted and fluid-attenuated inversion-recovery images did not reveal abnormal intensities in the cerebellum and pons.

In patient 1, T2-weighted images revealed diffuse high-intensity areas in cerebral white matter (Fig. 3a, d), but the T1-weighted images revealed a slow progressive loss of myelin (Fig. 3b, c, e, f). The volume of basal ganglia was preserved in all patients. Mild diffuse cerebral atrophy was observed only in patient 3.

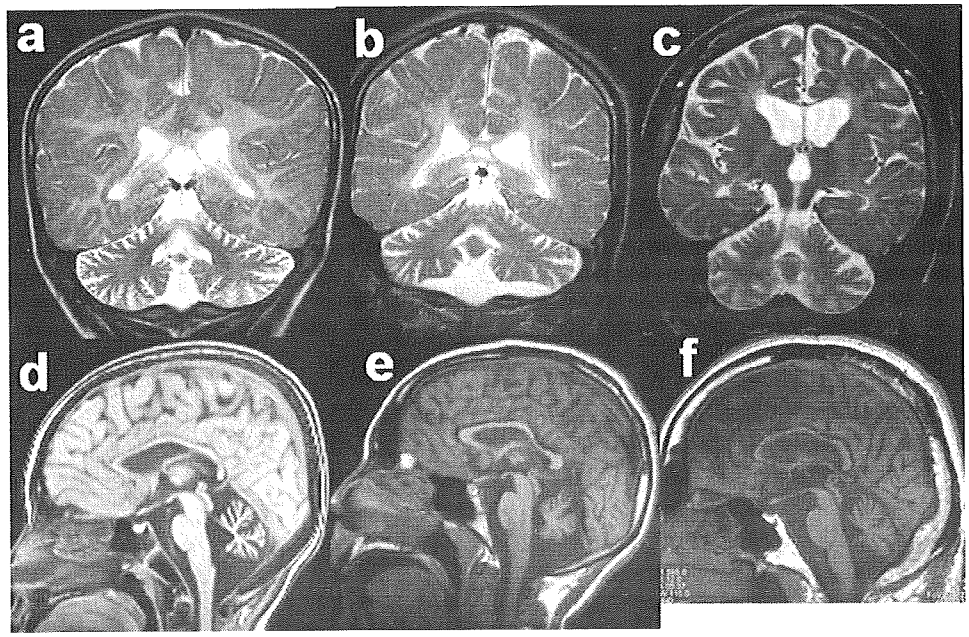

Fig. 1. T2-weighted coronal MRI (a, b, c) revealing high-intensity areas in the cerebral white matter and diffuse cerebellar cortical atrophy. Cerebral atrophy can be observed only in patient 3. T1-weighted sagittal MRI (d, e, f) reveals atrophy of the cerebellar vermis and hypoplasia of the myelinated corpus callosum in all cases (a, d: patient 1; b, e: patient 2; c, d: patient 3).

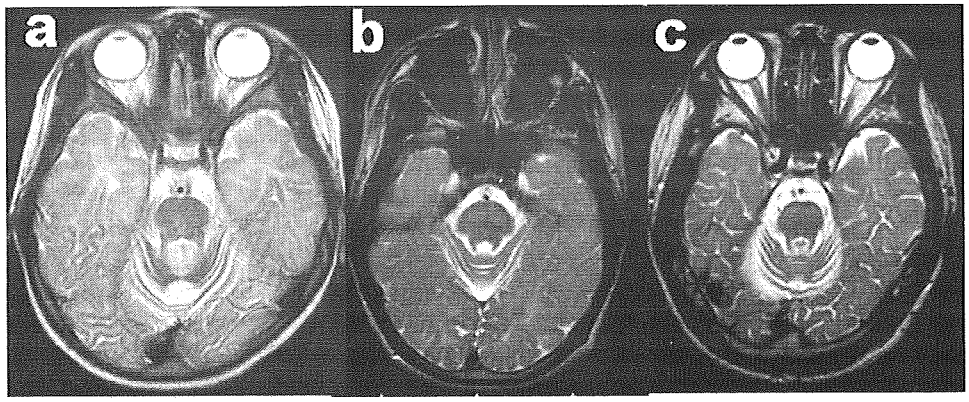

Fig. 2. T2-weighted axial MRI at the cerebellopontine level (a: patient 1; b: patient 2; c: patient 3). The cerebellar cortex is atrophic, and normal signal intensity can be seen in all three cases. Pons is slightly atrophic, but myelination appears normal in all cases.

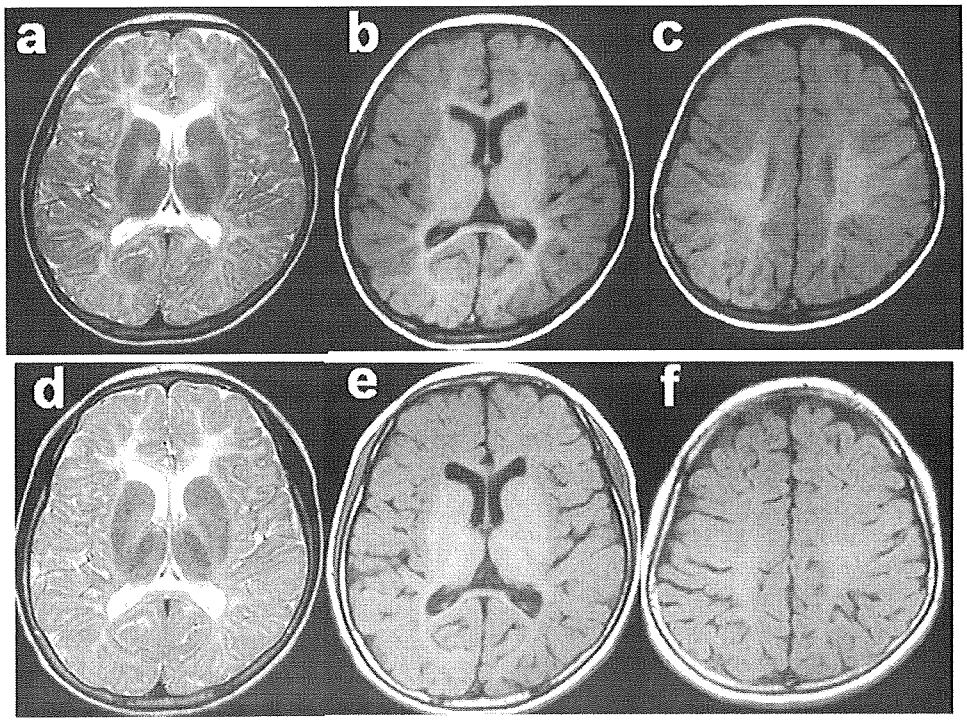

Fig. 3. Axial MRI of patient 1. At 4 years of age (above), diffuse high-intensity areas can be seen throughout the white matter in T2-weighted image (a) and high-intensity areas are evident in the central white matter in T1-weighted images (b, c), indicating diffuse hypomyelination. At 11 years of age (below), T2-weighted image shows findings (d) identical to that seen at 4 years of age. T1-weighted images show that the area of myelinated white matter is reduced (e, f) compared with that seen at 4 years of age, indicating a progressive disorder. The volume of basal ganglia is normal.

3.3. MRS

MRS of the cerebral white matter revealed that the lactate/lipid peak, the *N*-acetylaspartate (NAA)/creatine (Cr) ratio, and the choline/Cr ratio were normal in all patients.

4. Discussion

The common symptoms in the patients described in this study were ataxic gait, mild or moderate intellectual deterioration, and a very mild progressive clinical course. Common MRI findings included diffuse high-intensity areas in the cerebral white matter in T2-weighted images, mild cerebellar atrophy, and hypoplasia of the corpus callosum. MRI findings in all patients indicated hypomyelination due to the diffuse high-intensity signal throughout the abnormal area in the cerebral white matter in T2-weighted images, and the relatively high-intensity area in T1-weighted images. Biochemical and/or genetic studies excluded disorders characterized by diffuse hypomyelination such as Peliza-

Table 2
MRI findings in various diffuse hypomyelination syndromes

Syndrome	Cerebral white matter	Atrophy of the basal ganglia	Atrophy of the cerebellum	Atrophy of the corpus callosum	Specific features
H-ABC	Diffuse hypomyelination	(+)	(+)	(+) or (−)	Atrophy of the basal ganglia
4H	Diffuse hypomyelination	(−)	(+) or (−)	(+)	Hypogonadism Hypodontia Peripheral neuropathy
HH	Diffuse hypomyelination	(−)	(−)	(+) or (−)	Hypodontia
HCC	Diffuse hypomyelination	(−)	(−)	(+) or (−)	Cataract Peripheral neuropathy Hyccin deficiency
Present cases	Diffuse hypomyelination	(−)	(+)	(+)	Mild clinical course

H-ABC, hypomyelination with atrophy of the basal ganglia and cerebellum.
4H, hypomyelination with hypogonadotropic hypogonadism and hypodontia.
HH, hypomyelination and hypodontia.
HCC, hypomyelination and congenital cataract.

eus-Merzbacher disease, Salla disease, or Pelizaeus-Merzbacher-like syndrome [16,17].

MRI findings of diffuse cerebral hypomyelination have been described in other syndromes, including hypomyelination and congenital cataracts (HCC), hypomyelination with hypogonadotropic hypogonadism and hypodontia (4H), hypomyelination and hypodontia (HH), and hypomyelination with atrophy of the basal ganglia and cerebellum (H-ABC). These syndromes have characteristic findings that occur along with diffuse cerebral hypomyelination, such as congenital cataracts and peripheral neuropathy in HCC (no cerebellar atrophy); hypogonadotropic hypogonadism, hypodontia and peripheral neuropathy in 4H; hypodontia in HH; and cerebellar and basal ganglia atrophy in H-ABC.

MRI findings of the cerebral white matter in the patients described here were similar to the four syndromes listed above (Table 2), but further myelin loss was observed in T1-weighted images in patient 1 during follow-up. Identical MRI changes have been reported in some patients with H-ABC [10]. The patients in this study also had slow progressive clinical courses. Some patients with H-ABC have rapid progressive clinical courses [7,10]. Progression of clinical courses in the three patients was slower than that reported in patients with H-ABC. Changes in motor ability in our patients were similar to those seen in HCC patients. Except for one case, all HCC patients lost the ability to walk with support by 20 years of age [14].

The genetic abnormality responsible for HCC is caused by defects in a gene that encodes a new protein named "hyccin" [13]. The function of hyccin has not been identified, although it has putative transmembrane segments suggesting membrane localization. RNA blot analysis shows that hyccin is expressed ubiquitously in the adult brain and lens. Genetic abnormalities have not been identified for H-ABC, 4H, or HH. It is possible that these disorders are caused by a similar protein deficiency, and that genes expressed in the cerebral white matter and/or peripheral nerve (at least in the cases of 4H [15] and HCC [14]) are involved.

Although a genetic abnormality was not found in our patients, we believe that they have another subset form of diffuse hypomyelination syndrome involving the cerebrum and cerebellum because of common MRI findings and clinical symptoms. The common MRI findings were diffuse cerebral hypomyelination, cerebellar atrophy, and corpus callosum atrophy without basal ganglia atrophy. The underlying genetic abnormalities responsible for the various diffuse cerebral hypomyelination syndromes have been discovered only for HCC; hence, the pathogenesis of these syndromes must be pursued at a genetic level to ascertain if these syndromes are independent.

Acknowledgement

The authors are very grateful to Dr Hitoshi Osaka at Kanagawa Children's Medical Center for analyzing the *PLP* and *GJP12* genes. This study was supported in part by the Research Grant (20A-14) for Nervous and Mental Disorders from the Ministry of Health, Labor and Welfare.

References

[1] van der Knaap MS, Breiter SN, Naidu S, Hart AA, Valk J. Defining and categorizing leukoencephalopathies of unknown origin: MR imaging approach. Radiology 1999;213:121–33.
[2] Schiffmann R, Moller JR, Trapp BD, Shih HH, Farrer RG, Katz DA, et al. Childhood ataxia with diffuse central nervous system hypomyelination. Ann Neurol 1994;35:331–40.
[3] van der Knaap MS, Barth PG, Gabreels FJ, Franzoni E, Begeer JH, Stroink H, et al. A new leukoencephalopathy with vanishing white matter. Neurology 1997;48:845–55.
[4] van der Knaap MS, Barth PG, Stroink H, van Nieuwenhuizen O, Arts WF, Hoogenraad F, et al. Leukoencephalopathy with swelling and a discrepantly mild clinical course in eight children. Ann Neurol 1995;37:324–34.

[5] Leegwater PA, Vermeulen G, Konst AA, Naidu S, Mulders J, Visser A, et al. Subunits of the translation initiation factor eIF2B are mutant in leukoencephalopathy with vanishing white matter. Nat Genet 2001;29:383–8.
[6] Leegwater PA, Yuan BQ, van der Steen J, Mulders J, Könst AA, Boor PK, et al. Mutations of MLC1 (KIAA0027), encoding a putative membrane protein, cause megalencephalic leukoencephalopathy with subcortical cysts. Am J Hum Genet 2001;68:831–8.
[7] van der Knaap MS, Naidu S, Pouwels PJ, Bonavita S, van Coster R, Lagae L, et al. New syndrome characterized by hypomyelination with atrophy of the basal ganglia and cerebellum. Am J Neuroradiol 2002;23:1466–74.
[8] Mercimek-Mahmutoglu S, van der Knaap MS, Baric I, Prayer D, Stoecker-Ipsiroglu S. Hypomyelination with atrophy of the basal ganglia and cerebellum (H-ABC). Report of a new case. Neuropediatrics 2005;36:223–6.
[9] Wakusawa K, Haginoya K, Kitamura T, Togashi N, Ishitobi M, Yokoyama H, et al. Effective treatment with levodopa and carbidopa for hypomyelination with atrophy of the basal ganglia and cerebellum. Tohoku J Exp Med 2006;209:163–7.
[10] van der Knaap MS, Linnankivi T, Paetau A, Feigenbaum A, Wakusawa K, Haginoya K, et al. Hypomyelination with atrophy of the basal ganglia and cerebellum: follow-up and pathology. Neurology 2007;69:166–71.
[11] Wolf NI, Harting I, Boltshauser E, Wiegand G, Koch MJ, Schmitt-Mechelke T, et al. Leukoencephalopathy with ataxia, hypodontia, and hypomyelination. Neurology 2005;64:1461–4.
[12] Wolf NI, Harting I, Innes AM, Patzer S, Zeitler P, Schneider A, et al. Ataxia, delayed dentition and hypomyelination: a novel leukoencephalopathy. Neuropediatrics 2007;38:64–70.
[13] Zara F, Biancheri R, Bruno C, Bordo L, Assereto S, Gazzerro E, et al. Deficiency of hyccin, a newly identified membrane protein, causes hypomyelination and congenital cataract. Nat Genet 2006;38:1111–3.
[14] Biancheri R, Zara F, Bruno C, Rossi A, Bordo L, Gazzerro E, et al. Phenotypic characterization of hypomyelination and congenital cataract. Ann Neurol 2007;62:121–7.
[15] Timmons M, Tsokos M, Asab MA, Seminara SB, Zirzow GC, Kaneski CR, et al. Peripheral and central hypomyelination with hypogonadotropic hypogonadism and hypodontia. Neurology 2006;67:2066–9.
[16] Uhlenberg B, Schuelke M, Ruschendorf F, Ruf N, Kaindl AM, Henneke M, et al. Mutations in the gene encoding gap junction protein α12 (connexin 46.6) cause Pelizaeus-Merzbacher-like disease. Am J Hum Genet 2004;75:251–60.
[17] Bugiani M, Al Shahwan S, Lamantea E, Bizzi A, Bakhsh E, Moroni I, et al. GJA12 mutations in children with recessive hypomyelinating leukoencephalopathy. Neurology 2006;67:273–9.